Title

Enhanced nitrogen incorporation by pulsed laser annealing of GaNxAs1-x formed by N ion implantation

Permalink

https://escholarship.org/uc/item/4qj4z3x5

Journal

Applied Physics Letters, 80(21)

Authors

Yu, K.M.
Walukiewicz, W.
Beeman, J.W.
et al.

Publication Date

2002-01-16

Enhanced Nitrogen Incorporation by Pulsed Laser Annealing of GaN_xAs_{1-x} Formed by N Ion Implantation

K. M. Yu, W. Walukiewicz, J. W. Beeman,

Materials Sciences Division, Lawrence Berkeley National Laboratory, Berkeley, California 94720

M. A. Scarpulla, O. D. Dubon

Materials Sciences Division, Lawrence Berkeley National Laboratory, and Department of Materials Sciences and Mineral Engineering, University of California, Berkeley, California 94720

M. R. Pillai, M. J. Aziz

Division of Engineering and Applied Sciences, Harvard University, Cambridge, MA 02138

ABSTRACT

We demonstrate that pulsed laser annealing followed by rapid thermal annealing greatly enhances incorporation of substitutional N in N^+-implanted GaAs. Films implanted to 1.8% N exhibit a fundamental band gap of 1.26eV (a band gap reduction of 160meV), corresponding to an N activation efficiency of 50%. The optical and crystalline quality of the synthesized film is comparable to GaN_xAs_{1-x} thin films of similar composition grown by epitaxial growth techniques. Compared to films produced by N^+ implantation and rapid thermal annealing only, the introduction of pulsed laser annealing improves N incorporation by a factor of five. Moreover, we find that the synthesized films are thermally stable up to an annealing temperature of 950°C.

PACS numbers: 71.20.Nr; 78.20.-e; 61.72.Vv; 81.40.Wx

The anomalously strong band gap bowing in GaN_xAs_{1-x} (>150meV for 1% of N) alloys has stimulated much interest in the properties and technological potential of this material [1-7]. The many unusual electronic and optical properties of GaN_xAs_{1-x} alloys are also observed in other III-N_x-V_{1-x} alloys such as InN_xP_{1-x}, GaN_xP_{1-x} and $Al_yGa_{1-y}N_xAs_{1-x}$.[8-12] Recently it was suggested that these III-N_x-V_{1-x} are members of the general class of highly mismatched alloys (HMAs) in which a small fraction of the metallic anions are replaced by more electronegative elements.[13] The large band gap bowing in HMAs can be explained by an anticrossing interaction between localized states of the more electronegative element and the extended states of the host semiconductor matrix [14,15]. Other examples of HMAs include ZnS_xSe_{1-x} ZnS_xTe_{1-x}, $ZnSe_xTe_{1-x}$ and the II-O_x-VI_{1-x} alloys [13,16].

Most reports to date on III-N_x-V_{1-x} alloys involve thin films grown by gas-source molecular beam epitaxy (MBE) or metalorganic chemical vapor deposition (MOCVD) techniques. The formation of GaN_xAs_{1-x} thin films by N^+ implantation in GaAs followed by rapid thermal annealing (RTA) has also been explored [11,17,18]. Using RTA an activation efficiency of only ~10 to15% is achievable for implanted N mole fractions (x_{imp}) less than 0.036. The highest active N fraction reported using this technique is x_{act} $\approx$0.004 for $x_{imp}\approx$0.036 [18].

Pulsed laser annealing (PLA) [19] of ion implanted Si and GaAs was studied extensively in the 1970s and 1980s [20, 21]. It involves the melting induced by pulsed laser of the implant-damaged or amorphized layer and its subsequent rapid epitaxial regrowth. Epitaxy is seeded at the solid-liquid interface by the crystalline bulk in a manner very similar to liquid phase epitaxy (LPE) but with the whole process occurring on a much shorter time scale, typically between 10^{-8}-10^{-6} second. It was shown that using the PLA method amorphous layers of GaAs formed by high dose implantation can be regrown into nearly perfect single crystals with electrical activities of dopants well above those achievable by furnace annealing [21]. In this letter we report on our efforts to increase the N incorporation in N^+-implanted GaAs using pulsed laser annealing followed by RTA.

The details of the N^+ implantation conditions in GaAs can be found in Reference 18. Briefly, semi-insulating GaAs substrates were implanted with N^+ at multiple energies creating ~3000Å layers of GaAs with a uniform N concentration of ~$3.9x10^{20}cm^{-3}$. This corresponds to an x_{imp}~0.018. It is important to recognize that only a fraction of the implanted N will occupy As sublattice sites (N_{As}) after annealing and thus become "active" (x_{act}).

The N^+-implanted GaAs samples were pulsed-laser melted in air using an XeCl excimer laser (λ=308nm) with pulse duration ~30ns. After passing through a multi-prism homogenizer, the fluence at the sample ranged between 0.3 and 0.8J/cm^2. The melt duration (τ_{melt}) was determined by monitoring the time resolved reflectivity (TRR) of the samples using an argon-ion laser. TRR confirmed that the GaAs samples were indeed melted with τ_{melt} of approximately 150 ns and 345 ns for laser fluences of 0.35 and 0.79 J/cm^2, respectively. Some of the samples were rapid thermally annealed (RTA) after the PLA at temperatures between 800 and 950°C for 10 seconds in flowing N_2.

The crystalline structure of the GaN_xAs_{1-x} samples was studied by channeling Rutherford backscattering spectrometry (c-RBS) in the <100> direction. The band gap of the films was measured using photomodulated reflectance (PR) at room temperature. Radiation from a 300W halogen tungsten lamp dispersed by a 0.5m monochromator was focused on the samples as a probe beam. A chopped HeCd laser beam (λ=442 nm or 325nm) provided the photomodulation. PR signals were detected by a Si photodiode using a phase-sensitive lock-in amplification system. The values of the band gap and the line width were determined by fitting the PR spectra to the Aspnes third-derivative functional form. [22]

Fig. 1 shows the c-RBS spectra from unimplanted GaAs and N^+-implanted GaAs samples as-implanted and after PLA with pulse fluence of 0.35 J/cm^2 (PLA) and subsequently RTA at 950ºC after PLA (PLA+950ºC RTA). The <100> aligned spectrum from the as-implanted GaAs sample reveals that the sample is highly damaged yet still crystalline after N^+ implantation. The high dechanneling and the absence of a direct scattering peak in the spectrum suggest that the majority of the damage present in the top 300nm layer of the sample consists of extended crystalline defects [23].

The <100> aligned spectrum from the sample exposed to a pulse fluence of 0.35J/cm^2 shows a thin layer (~100nm) of good crystalline materials on a defective underlayer. The high dechanneling rate in the region deeper than ~100nm suggests that only the top 100nm of GaAs was melted and epitaxially regrown from the liquid phase. Since the underlying GaAs was defective, a high concentration of defects is expected to accumulate at the regrowth interface. This gives rise to the high dechanneling rate between 100 and 200 nm. In order to heal these interfacial defects observed in the PLA sample, RTA was carried out for 10s in the temperature range of 800-950°C. c-RBS measurements on the PLA+950°C RTA sample shows much improved crystalline quality.

Photomodulated reflectance (PR) measurements of the sample subjected only to PLA do not show any clear optical transition. This is consistent with the c-RBS results that show higher yields for this sample than the unimplanted sample, indicating that the regrown layer is still defective. Distinct optical transitions are observable only in the PLA samples after RTA at temperatures higher than 800ºC. Fig. 2 shows a series of PR spectra from samples processed by PLA and RTA together with an unimplanted GaAs and an N^+-implanted GaAs sample subjected only to RTA at 800°C. PR spectra from the laser melted and RTA (PLA+RTA) samples exhibit several well-resolved interband transitions that are distinctly different in energy from the fundamental band gap transition in the unimplanted GaAs (E_o). The main spectral feature at 1.26eV observed in all of the PLA+RTA samples is attributed to a GaN_xAs_{1-x} layer formed via epitaxial regrowth from the melt. The line width of this transition narrows as the RTA temperature increases, suggesting that the quality of this GaN_xAs_{1-x} layer improves with RTA temperature, which is in good agreement with the c-RBS results.

It has been demonstrated that the band gap reduction in III-N_xV_{1-x} alloys can be explained quantitatively by an anticrossing interaction between localized N-states and the extended states of the host semiconductor matrix [13-15]. This interaction splits the conduction band of the alloy into two subbands. The downward shift of the lower subband (E_-) is responsible for the reduction of the fundamental band gap, and optical transitions from the valence band to the upper subband account for the high-energy edge (E_+). Using this band anticrossing (BAC) model we calculate the active N content to be 0.9% (i.e. x=0.009 in GaN_xAs_{1-x}) for the measured band gap of 1.26eV. From Fig. 2 the upper subband edge energy E_+ is found to be approximately 1.81eV, which is in very good agreement with the calculated value.

Another prominent feature is observed around 1.4eV in the PR spectra of the PLA+RTA samples. This transition exhibits a slight blueshift from 1.36 to 1.4 eV as the RTA temperature increases from 800°C to 950°C. Since the N^+-implanted GaAs region is ~300nm thick and the laser melted region is estimated from c-RBS to be only ~100 nm, the underlying N-containing layer is expected to be similar to samples subjected to RTA only. Indeed, the broad line shape and the position of this transition are similar to those from a GaN_xAs_{1-x} layer formed by RTA alone. Furthermore, this 1.4eV transition is much weaker when the 325nm laser line is used for the photomodulation (top spectrum in Fig. 2). This result is indicative of a deep layer considering that the penetration depth of 325nm radiation in GaAs is only ~1/3 that of 442nm photons. Therefore, this feature at ~1.4eV is believed to arise from the deeper (>100nm) N-containing layer that did not undergo melting and rapid LPE regrowth. The significant broadening of the transition can be attributed to the tails of the N distribution and remaining implantation damage [12]. The N incorporated in this layer annealed entirely in the solid phase is estimated to be <0.1% after RTA at 950°C [17,18].

The value of the band gap of the laser melted layers does not change significantly even at RTA temperature of 950ºC, suggesting that the substitutional nitrogen (N_{As}) in these layers appears are thermally stable. We speculate that the extremely short duration of the laser melting and regrowth process inhibits the formation of nitrogen related voids, which have recently been observed in samples formed by N^+-implantation followed by RTA only [24]. The process of rapid melting and solidification may result in a complete local rearrangement of the atom sites leading to the formation of strong Ga-N bonds, thus stabilizing N atoms on the anion sites. The subsequent, lower temperature RTA cannot break these bonds but can improve the overall crystal quality by an atomic diffusion and rearrangement of the lower energy defects. In MOCVD grown GaN_xAs_{1-x} layers, N atoms on As sites are also found to be thermally stable at RTA at 950ºC [25].

Fig. 3 shows a comparison of the PR spectra of two samples exposed to different laser fluences (0.35 and 0.79J/cm^2) and RTA at 950ºC. The PR spectrum from the sample exposed to the higher fluence exhibits a much reduced intensity for the transition at ~1.4eV, which is consistent with the c-RBS result showing that the entire N^+-implanted layer was melted and has regrown epitaxially. However, the fundamental band gap of the layer in this sample is 1.305eV, a value significantly higher than that of the sample exposed to a fluence of 0.35J/cm^2. The amount of N_{As} in this sample is estimated by the BAC model to be $x \approx 0.005$. This lower content of substitutional N may be due to the longer duration of the melt associated with the higher fluence (345 ns compared to 150 ns) which would enable N atoms to migrate to the surface or coalesce to form bubbles (i.e., N-related voids). Transmission electron microscopy experiments are underway to provide more detailed information on defects and the microstructure of the annealed layers.

In conclusion we have demonstrated an effective new method to synthesize GaN_xAs_{1-x} alloys. We have shown that thin films of GaN_xAs_{1-x} with N content on the order 1% can be synthesized by N^+ implantation followed by a combination of pulsed laser annealing and rapid thermal annealing. Compared to GaN_xAs_{1-x} films synthesized by N^+ implantation and rapid thermal annealing only, the laser melting process improves the incorporation of substitutional N by a factor of five and enhances the thermal stability of N to a level similar to that observed for films grown by MOCVD.

This work is part of “Photovoltic Materials Focus Area” in the DOE Center of Excellence for the Synthesis and Processing of Advanced Materials, Office of Science, Office of Basic Energy Science, Division of Materials Sciences and Engineering, of the U.S. Department of Energy under Contract No.DE-AC03-76SF00098. MAS acknowledges support from an NSF graduate research fellowship. The work at Harvard was supported by NASA grant # NAG8-1680.

REFERENCES

1. S. Sakai, Y. Ueta and Y. Terauchi, *Jpn. J. Appl. Phys*. **32**, 4413 (1993).
2. M. Kondow, K. Uomi, K. Hosomi, and T. Mozume, *Jpn. J. Appl. Phys*. **33**, L1056 (1994).
3. K. Uesugi, N. Morooka, and I. Suemune, *Appl. Phys. Lett. **74***, 1254(1999).
4. J. F. Geisz, D. J. Friedman, J. M Olson, S. R. Kurtz, and B. M. Keyes, *J. Cryst. Growth* **195**, 401 (1998).
5. M. Kondow, T. Kitatani, M. C. Larson, K. Nakahara, K. Uomi and H. Inoue, *J. Crystal Growth* **188**, 255 (1998).
6. D. J. Friedman, J. F. Geisz, S. R. Kurtz, D. Myers and J. M Olson, *J. Cryst. Growth* **195**, 409(1998).
7. S. R. Kurtz, A.A. Allerman, E.D. Jones, J.M. Gee, J.J. Banas, and B.E. Hammons, *Appl. Phys. Lett*. **74**, 729(1999).
8. J. N. Baillargeon, K. Y. Cheng, G. E. Hofler, P. J. Pearah and K. C. Hsieh, *Appl. Phys. Lett*. **60**, 2540 (1992).
9. W. Shan, W. Walukiewicz, K. M. Yu, J. Wu, J. W. Ager, E. E. Haller, H. P. Xin, and C. W. Tu, *Appl. Phys. Lett*. **76**, 3251 (2000).
10. W. G. Bi and C. W. Tu, *J. Appl. Phys*. **80**, 1934 (1996).
11. W. Shan, W. Walukiewicz, K. M. Yu, J. W. Ager III, E. E. Haller, J. F. Geisz, D. J. Friedman, J. M. Olson, Sarah R. Kurtz, and K. Nauka,Phys. Rev. **B62**, 4211 (2000).
12. W. Shan, K. M. Yu, W. Walukiewicz, J. W. Ager, E. E. Haller and M. C. Ridgway, *Appl. Phys. Lett*. **75**, 1410 (1999).
13. W. Walukiewicz, W. Shan, K. M. Yu, J. W. Ager III, E. E. Haller, I. Miotlowski, M. J. Seong, H. Alawadhi, and A. K. Ramdas, *Phys. Rev. Lett*. **85**, 1552 (2000).
14. W. Shan, W. Walukiewicz, J. W. Ager III, E. E. Haller, J. F. Geisz, D. J. Friedman, J. M. Olson, and S. R. Kurtz, *Phys. Rev. Lett*. **8**2, 1221(1999).

15. W. Walukiewicz, W. Shan, J. W. Ager III, D. R. Chamberlin, E. E. Haller, J. F. Geisz, D. J. Friedman, J. M. Olson, and S. R. Kurtz, in *Photovoltaics for the 21st Century*, edited by V. K. Kapur, R. D. McDonnell, D. Carlson, G. P. Ceasar, A. Rohatgi (Electrochemical Society Press, Pennington, 1999) p. 190.
16. K. M. Yu, W. Walukiewicz, J. Wu, J. W. Beeman, J. W. Ager, E. E. Haller, I. Miotkowski, A. K. Ramdas, and P. Becla, Appl. Phys. Lett. **80**, 1571 (2002).
17. K. M. Yu, W. Walukiewicz, W. Shan, J. Wu, J. Beeman, J. W. Ager III, E. E. Haller, and M. C. Ridgway, Mater. Res. Soc. Symp. Proc. **647**, O13.3.1/R8.3.1 (2001).
18. K. M. Yu, W. Walukiewicz, J. Wu, J. W. Beeman, J. W. Ager III, E. E. Haller, W. Shan, H. P. Xin, C. W. Tu, and M. C. Ridgway, J. Appl. Phys. **90**, 2227 (2001).
19. Both the terms pulsed laser melting (PLM) and pulsed laser annealing (PLA) have been used in the literature to describe the same annealing phenomena in semiconductors. In this paper we used the term PLA to describe the process of rapid melting and solidification due to the short laser pulses. We note that PLA here does not refer to annealing in the solid state without melting such as that in the low-power pulsed laser annealing (LPPLA) process.
20. C. W. White and P. S. Peercy, eds., *Laser and Electron Beam Processing of Materials* (Academic Press, New York, 1980).
21. J. S. Williams in *Laser Annealing of Semiconductors*, J. M. Poate and J. W. Mayer, eds., p. 385 (Academic Press, New York, 1982).
22. D. E. Aspnes, *Surf. Sci.* **37**, 418 (1973).
23. L. C. Feldman, J. W. Mayer, and S. T. Picraux, *Materials Analysis by Ion Channeling* (Academic, New York, 1982).
24. J. Jasinski, K. M. Yu, W. Walukiewicz, Z. Liliental-Weber and J. Washburn, " Appl. Phys. Lett. **79**, 931 (2001).
25. K. M. Yu, unpublished data.

FIGURE CAPTIONS

Fig. 1 Channeling Rutherford backscattering spectra (c-RBS) taken in the <100> axial direction from N^+-implanted GaAs samples as-implanted , annealed with laser pulse fluence of 0.35 J/cm^2 (LA) and with subsequent RTA at 950ºC for 10s after PLA (PLA+950ºC RTA). The <100> aligned and random spectra from an unimplanted GaAs sample are also shown.

Fig. 2 A series of photomodulated reflectance (PR) spectra (λ=442nm modulation) from N^+-implanted GaAs after PLA (laser fluence =0.35J/cm^2) and RTA at different temperatures. The top most spectrum was obtained from a PLA+950ºC RTA sample using the 325-nm line of a HeCd laser as a modulation source. All other spectra were obtained using the 442 nm line. Spectra from unimplanted GaAs, and N^+-implanted GaAs subjected to RTA at 800°C are also shown for comparison

Fig. 3 A comparison of the PR spectra obtained from samples exposed to laser pulse fluences of 0.35 and 0.79J/cm^2 and subsequently annealed at 950 °C for 10 s.

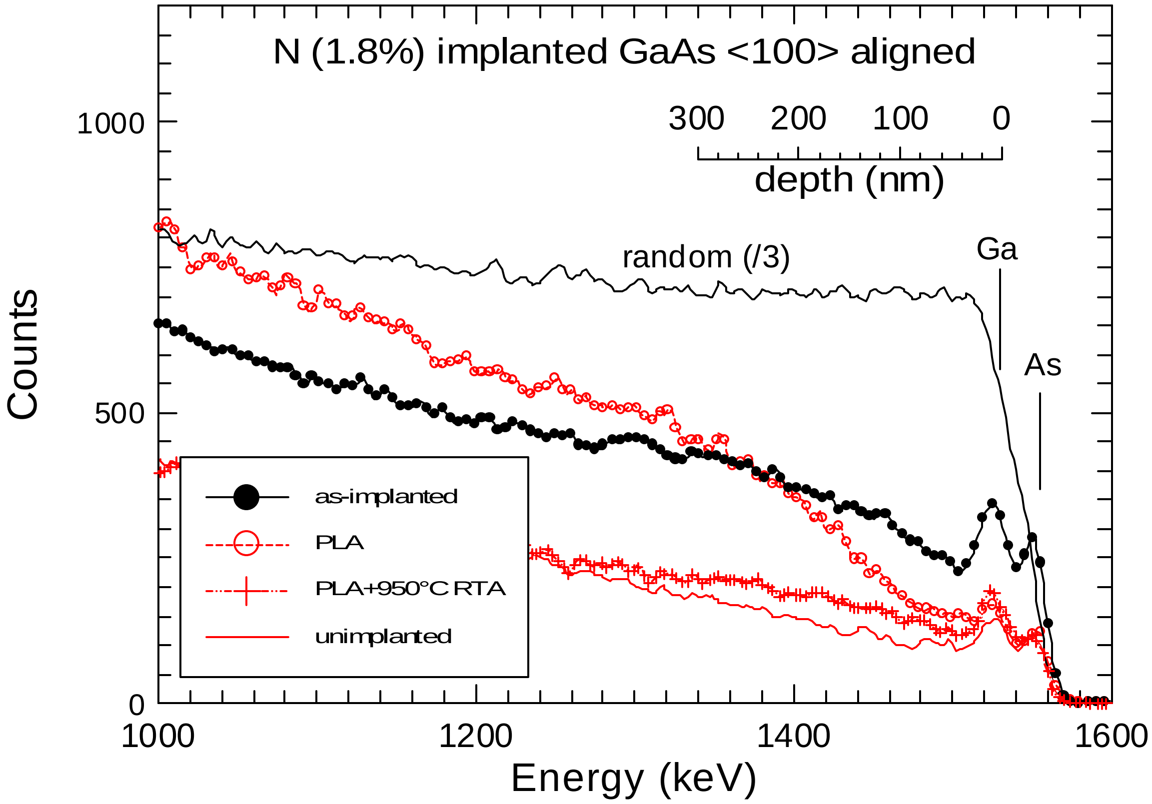
N (1.8%) implanted GaAs <100> aligned
300
200
100
0
depth (nm)
random (/3)
Ga
As
as-implanted
PLA
PLA+950°C RTA
unimplanted
Counts
0
500
1000
1000
1200
1400
1600
Energy (keV)

Fig. 1

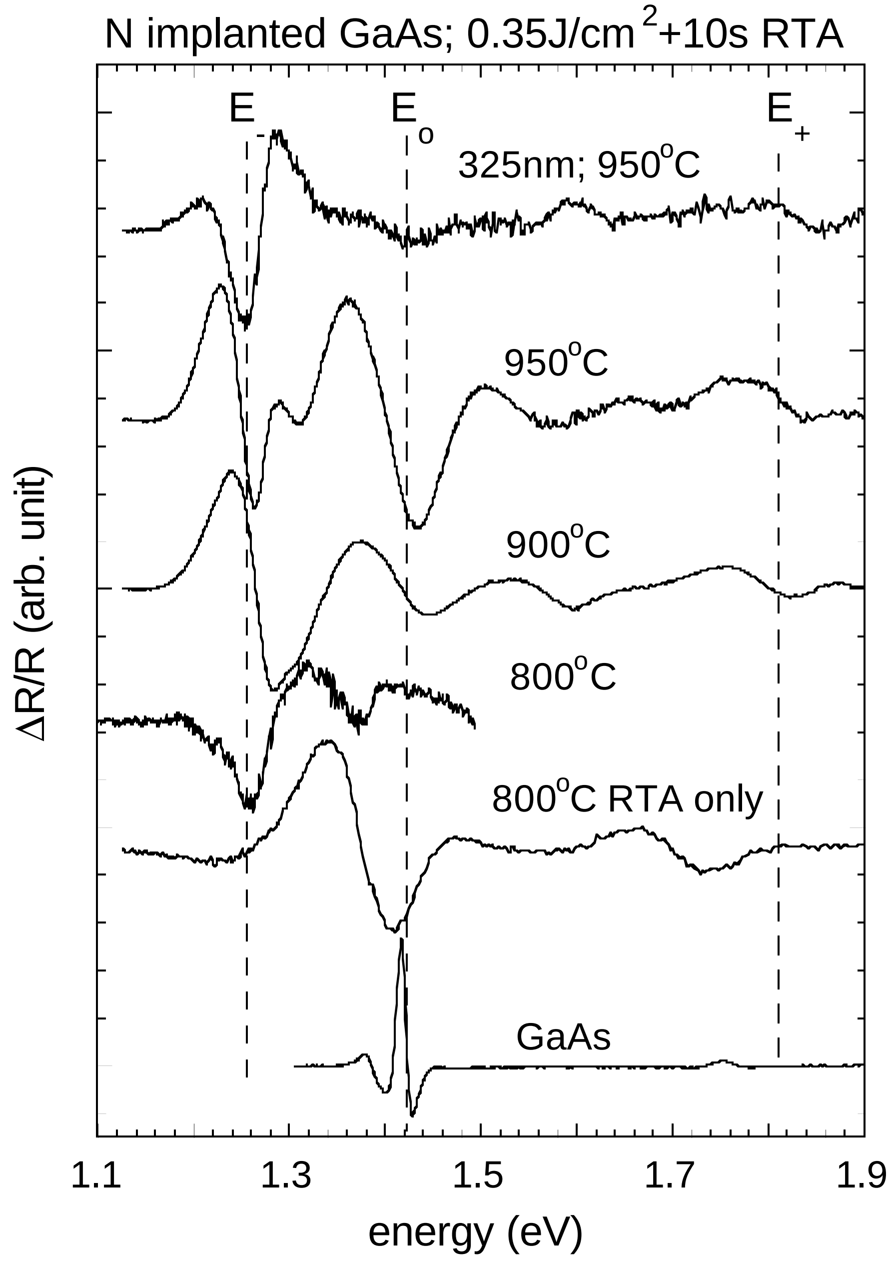
N implanted GaAs; 0.35J/cm^2+10s RTA
E_-
E_o
E_+
325nm; 950°C
950°C
900°C
800°C
800°C RTA only
GaAs
ΔR/R (arb. unit)
1.1
1.3
1.5
1.7
1.9
energy (eV)

Fig. 2

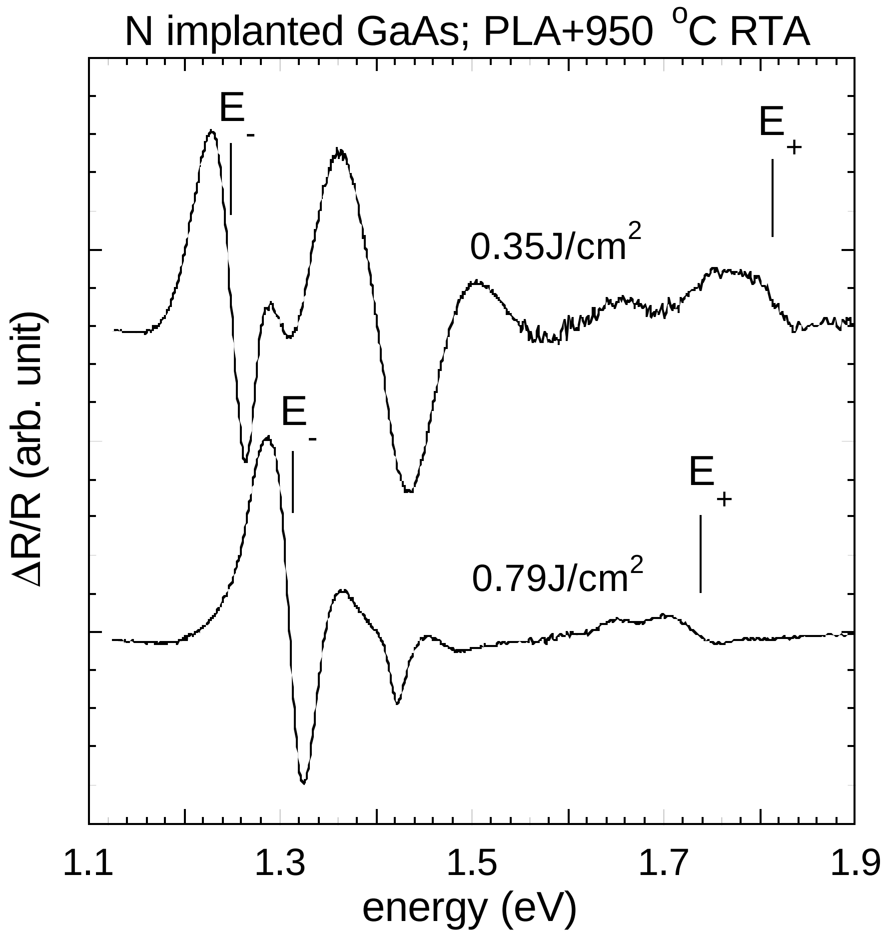
N implanted GaAs; PLA+950 °C RTA
ΔR/R (arb. unit)
energy (eV)
1.1
1.3
1.5
1.7
1.9
E-
E+
0.35J/cm2
E-
E+
0.79J/cm2

Fig. 3